Journal of Nuclear Medicine, published on December 13, 2019 as doi:10.2967/jnumed.119.234906

Histologically-confirmed diagnostic efficacy of ^{18}F-rhPSMA-7 positron emission tomography for N-staging of patients with primary high risk prostate cancer

Markus Kroenke[1], Alexander Wurzer[2], Kristina Schwamborn[3], Lena Ulbrich[1], Lena Jooß[1], Tobias Maurer[4], Thomas Horn[5], Isabel Rauscher[1], Bernhard Haller[6], Michael Herz[1], Hans-Jürgen Wester[2], Wolfgang A Weber[1], Matthias Eiber[1].

1 Technical University of Munich, School of Medicine, Klinikum rechts der Isar, Department of Nuclear Medicine;

2 Technical University of Munich, Chair of Radiopharmacy;

3 Technical University of Munich, School of Medicine, Klinikum rechts der Isar, Institute of Pathology, Technical University of Munich;

4 Martini-Klinik and Department of Urology, University Hospital Hamburg Eppendorf

5 Technical University of Munich, School of Medicine, Klinikum rechts der Isar, Department of Urology;

6 Technical University of Munich, School of Medicine, Institute of Medical Informatics, Statistics and Epidemiology.

Corresponding author:

Matthias Eiber, Klinikum rechts der Isar, Ismaninger Straße 22, 81675 Munich, GERMANY, Phone +49.89.4140.4549, Fax +49.89.4140.7431, Email matthias.eiber@tum.de

First author:

Markus Kroenke, Klinikum rechts der Isar, Ismaninger Straße 22, 81675 Munich, GERMANY, Phone +49.89.4140.2621, Fax +49.89.4140.7431, Email markus.kroenke@tum.de

Conflicts of interest:

Patent application for rhPSMA (HJW, AW and ME). HJW and ME received funding from the SFB 824 (DFG Sonderforschungsbereich 824, Project B11) from the Deutsche Forschungsgemeinschaft, Bonn, Germany and Blue Earth Diagnostics Ltd, Oxford, UK (Licensee for rhPSMA) as part of an academic collaboration. HJW is founder, shareholder and advisor board member of Scintomics GmbH, Fuerstenfeldbruck, Germany. ME and WW are consultants for Blue Earth Diagnostics Ltd. No other potential conflicts of interest relevant to this article exist.

Wordcount: 4817

Running title: ^{18}F-rhPSMA-7 PET for primary N-staging

Abstract

296/350 words

^{18}F-rhPSMA-7 is a novel prostate specific membrane antigen (PSMA)- -ligand for positron emission tomography (PET) imaging. Here, we present data from a retrospective analysis using PET/computed tomography (CT) and PET/magnetic resonance imaging (MRI) exams to investigate the efficacy of ^{18}F-rhPSMA-7 PET for primary N-staging of patients with prostate cancer compared with morphological imaging (CT]MRI) and validated by histopathology.

Methods

Data from 58 patients with high risk prostate cancer (according to D'Amico) who were staged with ^{18}F-rhPSMA-7 PET/CT or PET/MRI at our institution between July 2017 and June 2018 were reviewed. The patients had a median pre-scan PSA value of 12.2 ng/mL (range, 1.2–81.6 ng/mL). The median injected activity of ^{18}F-rhPSMA-7 was 327 MBq (range, 132–410 MBq), with a median uptake time of 79.5 min (range, 60–153 min). All patients underwent subsequent radical prostatectomy and extended pelvic lymph node dissection. The presence of lymph node metastases was determined by an experienced reader independently for both the PET and morphological datasets using a template-based analysis on a 5-point scale. Patient-level and template-based results were both compared to histopathological findings.

Results

Lymph node metastases were present in 18 patients (31.0%) located in 52 of 375 templates (13.9%). Receiver operating characteristic analyses showed ^{18}F-rhPSMA-7 PET to perform

significantly better than morphological imaging on both patient and template-based analyses (Area under curves of 0.858 vs. 0.649, p=0.012 and 0.765 vs. 0.589, p<0.001, respectively). On patient-based analyses, the sensitivity, specificity and accuracy of ^{18}F-rhPSMA-7 PET were 72.2%, 92.5% and 86.2%, and those of morphological imaging 50.0%, 72.5% and 65.5%, respectively. On template-based analyses, the sensitivity, specificity and accuracy of ^{18}F-rhPSMA-7 PET were 53.8%, 96.9% and 90.9%, respectively, and those of morphological imaging were 9.6%, 95.0% and 83.2%, respectively.

Conclusion

^{18}F-rhPSMA-7 PET is superior to morphological imaging for N-staging of high risk primary prostate cancer. The efficacy of ^{18}F-rhPSMA-7 is similar to published data for ^{68}Ga-PSMA-11.

Keywords

Hybrid imaging; lymph nodes; N-staging; positron emission tomography (PET); prostate cancer; prostate-specific membrane antigen (PSMA).

INTRODUCTION

Prostate cancer (PC) is a leading cause of male cancer-related death worldwide (1). Determining the presence and extent of disease at primary diagnosis is important in order to accurately predict prognosis and to define the optimal treatment strategy (2-4). Lymph node metastases may be detected in up to 25% of patients with PC and are correlated with the risk for recurrence and associated with overall survival (5-7).

The current gold standard for N-staging is pelvic lymphadenectomy, although this technique cannot evaluate regions outside the surgical field, and is associated with morbidity and complications (8,9). While cross-sectional imaging with computed tomography (CT) or magnetic resonance imaging (MRI) and also positron emission tomography (PET) with choline-based tracers are associated with low sensitivity (10,11), prostate specific membrane antigen (PSMA)-ligand PET is increasingly used for primary staging of PC. It outperforms cross-sectional imaging (12) and has reported sensitivity in the range 33–99% with consistently high specificity of over 90% (13).

^{18}F-labelled PSMA radiotracers are under clinical evaluation and offer a number of potential advantages such as a longer half-life, larger batch production and lower positron range compared with their ^{68}Ga-labelled counterparts. Promising results for primary staging have been demonstrated in a preliminary case series investigating ^{18}F-PSMA-1007 (14). Radiohybrid PSMA (rhPSMA) ligands are a new class of theranostic PSMA-targeting agents that can be efficiently labeled with ^{18}F and radiometals such as ^{68}Ga or ^{177}Lu (JNM submitted 2019/234922). The lead compound in this class, ^{18}F-rhPSMA-7 shows favorable biodistribution

with low bladder retention, fast kinetics and encouraging first-in-men data (JNM submitted 2019/234609).

The aim of this retrospective analysis was to evaluate the diagnostic performance of ^{18}F-rhPSMA-7 PET for primary N-staging of patients with high risk PC compared with cross-sectional imaging and validated by histopathology.

MATERIALS AND METHODS

Patients

Data from all patients meeting the D'Amico criteria for high-risk PC (15) who underwent ^{18}F-rhPSMA-7 PET/CT or PET/MRI and subsequent radical prostatectomy and extended pelvic lymph node dissection at our clinic between July 2017 and June 2018 were reviewed retrospectively. All patients who had received neoadjuvant treatment (either before or after the PET) or had not undergone radical prostatectomy with extended pelvic lymphadenectomy at our institution were excluded. In total, 58 patients were enrolled (Fig 1). Patients' characteristics are presented in Table. 1.

All patients gave written, informed consent for the purpose of anonymized evaluation and publication of their data. The retrospective analysis was approved by the local Ethics Committee (permit 290/18S). The administration of ^{18}F-rhPSMA-7 complied with The German Medicinal Products Act, AMG §13 2b, and the responsible regulatory body (Government of Oberbayern).

^{18}F-rhPSMA-7 Synthesis, Administration and PET Imaging

^{18}F-rhPSMA-7 was synthesized as reported previously (JNM submitted 2019/234922). ^{18}F-rhPSMA-7 (median activity, 327 MBq, range 132–410 MBq) was administered as an intravenous bolus a median of 79.5 (range, 60–153) minutes prior to scanning. Thirty-nine patients underwent a contrast-enhanced ^{18}F-rhPSMA-7 PET/CT (Biograph mCT flow, Siemens Medical Solutions, Erlangen, Germany). Nineteen patients underwent ^{18}F-rhPSMA-7 PET/MR (Biograph mMR, Siemens Medical Solutions, Erlangen, Germany). The PET/CT and PET/MR acquisition were conducted as described previously (16,17). All patients received diluted oral contrast (300 mg Telebrix).

All PET scans were acquired in 3D mode with an acquisition time of 2 min per bed position in flow technique (equals 1.1 mm/s) for PET/CT and 4 min per bed position for PET/MR. Emission data were corrected for randoms, dead time, scatter, and attenuation and were reconstructed iteratively by an ordered-subsets expectation maximization algorithm (four iterations, eight subsets) followed by a post-reconstruction smoothing Gaussian filter (5 mm full width at one-half maximum).

Image Analysis

All ^{18}F-rhPSMA-7 PET/CT and PET/MR datasets were reviewed by experienced physicians (ME (board certified radiologist and nuclear medicine specialist) and MK (board certified nuclear medicine specialist)) who were blinded to the post-operative histology results. Results

were determined by consensus. In a first step, the anatomical data using the diagnostic contrast enhanced CT dataset (PET/CT exams) and pelvic axial T2 TSE and the whole-body axial T2 haste sequences (PET/MR exams) were analyzed. In a second step, after an interval of at least 4 weeks, a second read of the corresponding ^{18}F-rhPSMA-7 PET scan was carried out. For the latter, anatomical images were used only for anatomical allocation of a suspicious focal increased uptake to the corresponding lymph node template. In both reading sessions, each template was rated in PET and CT or MR using a five-point Likert scale (1: tumor manifestation 2: probably tumor manifestation, 3: equivocal, 4: probably benign, 5: benign, detailed criterial are in the Supplemental inforamtion).

Histopathology

During surgery, an extended pelvic lymphadenectomy was performed as recently described (18,19). The following standard lymph node templates were collected separately: right/left common iliac vessel, right/left internal iliac vessel, right/left external iliac vessel, right/left obturator fossa. When preoperative imaging showed ^{18}F-rhPSMA-7 PET-positive lymph nodes outside these regions, additional templates (e.g. presacral/pararectal) were resected. Uropathologists were not aware of the pre-operative imaging results.

Statistical Analysis

Histopathological results from resected lymph nodes were correlated with the results of cross-sectional imaging (MR or CT) and ^{18}F-rhPSMA-7 PET in a patient- and template-based manner.

Overall diagnostic accuracy of patient-level data was assessed using receiver operating characteristics (ROC) analyses. ROC curves were calculated for both modalities (^{18}F-rhPSMA-7 PET, morphological imaging). Areas under the ROC curves (AUCs) with 95% confidence intervals were calculated and compared to each other. For patient–based analysis, the method by DeLong et al. (20) was used, the approach proposed by Obuchowski (21) as considered for template-based analyses to account for correlations of multiple assessments within one patient.

In order to estimate sensitivities, specificities and accuracies, a dichotomization of the semi-quantitative 5-scale rating for PET and CT/MR was performed in order to conduct statistical analyses. The Youden-Index (sensitivity + specificity - 1) was used to determine the best cut-off for this analysis. In the patient-based analyses, exact confidence intervals were estimated for these measures based on the binomial distribution (Clopper-Pearson intervals). For the template-based analyses, logistic generalized estimating equation models were fitted to the data to account for the correlation of multiple observations within the same patient (22,23). For estimation of sensitivities with associated confidence intervals, only templates with a positive histological result were included and the result of the diagnostic test was used as dependent variable.

To derive estimates for the specificities, a variable indicating whether a negative test result was observed, was used as dependent variable and only patients with a negative histopathological result were included. Accuracy was estimated in an intercept-only model with a dependent variable that indicated, whether the test result and the result of the

histopathological assessment agreed. For the generalized estimating equation model, an independent correlation structure was assumed. A significance level of 5% was considered for all tests. All statistical analyses were performed using the statistical software R (24), with its packages pROC (25) and geepack (26).

RESULTS

Histopathological Results and ROC Analysis

Lymph node metastases were present in 52 of 375 (13.9%) resected templates in 18 of the 58 patients (31%). ^{18}F-rhPSMA-7 PET revealed positivity of the local tumor in 57 (98.3%) patients. One patient showed evidence of distant lymph node metastases and bone metastases (1.9%).

On a patient-based analysis, ROC curves for ^{18}F-rhPSMA-7 PET showed an AUC of 0.858 (95% CI: 0.739–0.978) and for morphological imaging of 0.649 (95% CI: 0.492–0.805) for the detection of lymph node metastases (Fig 2a). On the template-based analysis, ROC curves for ^{18}F-rhPSMA-7 PET showed an AUC of 0.766 (95% CI: 0.697–0.834) and for morphological imaging alone of 0.589 (95% CI: 0.522–0.656) (Fig 2b). ^{18}F-rhPSMA-7 PET performed significantly better than morphological imaging alone on a patient- (difference in AUCs: 0.210, 95% CI: 0.046–0.373, p=0.012) and template-based analysis (difference in AUCs: 0.177, 95% CI: 0.104–0.249, p<0.001).

Based on the Youden-Index, scores of 1–3 on the Likert scale were regarded as positive, while scores 4 or 5 were considered as negative for morphological imaging. For ^{18}F-rhPSMA-7 PET scores of 1 or 2 were compared with scores of 3–5. A representative example is presented in Fig 3.

Diagnostic Performance n Patient-Based Analysis

Compared to histopathology, ^{18}F-rhPSMA-7 PET detected 13/18 patients with histological proven lymph node metastasis (sensitivity: 72.2%; 95% CI: 46.5–90.3%) while 3 of 40 patients without lymph node metastases were positive on ^{18}F-rhPSMA-7 PET (specificity: 92.5%; 95% CI: 79.6–98.4%). In total, ^{18}F-rhPSMA-7 PET showed an accuracy of 86.2% (95% CI: 74.6–93.9%) on a patient-based analysis (Table 2).

Morphological imaging alone correctly classified 9/18 patients as positive and 29/40 patients as negative for lymph node metastases, resulting in a sensitivity of 50.0% (95% CI, 26.0–74.0%), a specificity of 72.5% (95%CI, 56.1–85.4%) and an accuracy of 65.5% (95% CI, 51.9–77.5%) (Table 2).

In 35/58 (60.3%) PET and morphological imaging revealed concordant correct results (both true positive and true negative) and in five (8.6%) concordant false results. Discordant results were obtained in 18 patients (31%). Histological evaluation revealed PET imaging gave true positive and true negative results in 15 of these 18 patients (83.3%) with discordant results. ^{18}F-rhPSMA-7 PET reported both fewer false positives and false negatives than morphological imaging (3 vs. 11 and 5 vs. 9 patients, respectively).

Diagnostic Performance on Template-Based Analysis

Compared to histopathology, ^{18}F-rhPSMA-7 PET detected 28/52 templates with histological proven lymph node metastasis (sensitivity: 53.8%; 95% CI: 41.3–66.0%) while 10 of 323 templates without lymph node metastases were positive on ^{18}F-rhPSMA-7 PET (specificity: 96.9%; 95% CI: 91.4–98.9%). In total, ^{18}F-rhPSMA-7 PET showed an accuracy of 90.9 (95% CI: 85.7 – 94.4%) on a template-based analysis (Table 3).

Cross-sectional imaging alone correctly classified 5/52 templates as positive and 307/323 templates as negative for lymph node metastases, resulting in a sensitivity of 9.6% (95% CI, 4.5–19.3%), a specificity of 95.0% (95% CI, 92.2–96.9%) and an accuracy of 83.2% (95% CI, 76.5–88.3%) (Table 3).

The median size of the lymph node metastases not detected by ^{18}F-rhPSMA-7 PET was 4.5 mm (range: 0.3–15 mm). In two patients, histopathological false positive results of ^{18}F-rhPSMA-7 PET are challenged as described above.

Follow-up data retrieved from the post-operative clinical course for two patients revealed that lymph node templates which had been assigned as false positives with^{18}F-rhPSMA-7 PET were in fact true positives. In one patient with a persistent elevated PSA post-operatively, subsequent imaging four months later revealed persistent PSMA-ligand positivity in the initial region. A subsequent second targeted lymphadenectomy proved a lymph node metastasis (Supplemental Fig. 1). In a second patient, radiation planning (four months post-scan and after the operation) showed that the lesions in right obturator and left common iliac had

not been removed but decreased in size most likely due to start of androgen deprivation therapy after surgery. Updated statistics corrected for information are presented in Supplemental tab. 2.

DISCUSSION

The results of this retrospective analysis indicate that PET with the novel PSMA ligand, ^{18}F-rhPSMA-7, shows high diagnostic accuracy for N-staging in patients with primary high-risk PC. Its efficacy is superior compared with morphological imaging which is recommended by most guidelines (3).

Accurate localization of lesions, particularly to lymph nodes in patients with high-risk PC, is essential in order to optimize treatment planning. In particular, the identification of lymph node metastases is an unmet clinical need for non-invasive imaging given its adverse prognostic implications (4). Morphological imaging, using CT and MRI, has high variability in diagnostic performance for lymph node metastases (27). Characterization of lymph nodes solely by size is of limited use, as up to 80% of metastatic lymph nodes are normal-sized (< 8 mm) (28,29). Moreover, PET with , ^{11}C- or ^{18}F-labeled choline derivatives; is not recommended for first-line staging for patients with intermediate to high-risk PC (3).

Currently, PSMA-ligands are increasingly used in PC workup. They specifically target PC cells irrespective of their metabolic state (30) and offer a favorable lesion-to-background ratio

for detection of metastatic lymph nodes as normal lymphatic or retroperitoneal fatty tissue do not express PSMA.

The present results clearly indicate that ^{18}F-rhPSMA-7 PET performs significantly better than morphological imaging techniques. This difference is even more pronounced in the template-based analysis in which sensitivity of morphological imaging dropped to 9.6% (95% CI, 4.5–19.3%). Accuracy of ^{18}F-rhPSMA-7 PET was 86% and 91% vs. 66% and 83% for morphological imaging for patient and template-based analyses, respectively.

Compared with ^{68}Ga-PSMA-11, ^{18}F-rhPSMA-7 seems to perform equally well. In a sub-cohort of 88 high-risk patients, Maurer et al. reported a sensitivity, specificity and accuracy of 67%, 98% and 84% compared to 72%, 93% and 86% for ^{18}F-rhPSMA-7, respectively (31). Several meta-analyses have summarized published data on the performance of ^{68}Ga-PSMA-11 for N-staging; Hope et al summarized data from 266 patients for initial staging and reported a sensitivity, specificity, PPV, NPV and accuracy of 74%, 96%, 93%, 85% and 86%, respectively (32). Corfield et al (12) reported ranges for sensitivity, specificity, NPV and PPV of 33–92%, 64–91%, 83–96% and 80–96%, respectively across their analysis of over 200 patients. Similar pooled data have been recently published by von Eyben et al (33) and Perera et al (13). Despite a considerable range in sensitivity in the reported studies, specificity is consistently high in nearly all reports (Sup. Table. 1) as was observed in the current analysis for ^{18}F-rhPSMA-7. Only limited comparison with other ^{18}F-labelled PSMA-ligands is possible owing to a paucity of published data. For ^{18}F-DCFPyl, Gorin et al. reported data from a small prospective evaluation of 25 patients – a sensitivity and specificity of 71.4% (95% CI 29.0–96.3) and 88.9% (95% CI 65.3–

98.6), respectively (34). It is noteworthy that in our study the specificity on the template-based analysis is slightly underestimated due to the fact that two templates designated as false-positive were indeed true positives as indicated by follow-up data (adjusted statistics in supplemental table 2). The problem of incomplete resection of even pre-operatively known lymph node metastases has been recently reported (35). A potential solution could be the application of radio-guided surgery as known in recurrent disease (36).

Notably in our study, in nearly all patients (98.3%; 57/58) high ^{18}F-rhPSMA-7 uptake was expressed in the local tumor. One patient with a negative primary tumor was not found to have any lymph node metastases by histopathology. As known from ^{68}Ga-PSMA-11, size is critical for lesion detection (37). The present data show a similar mean size of negative lymph node templates to previous data reported by Maurer et al (3.5 mm) (31).

The novel PSMA-ligand, ^{18}F-rhPSMA-7, offers a number of advantages over more established PSMA-based tracers, such as ^{68}Ga-PSMA-11 and has already shown encouraging data for detection efficacy in biochemical recurrence (JNM submitted 2019/234914). The considerably longer half-life of 110 min yields the advantages of easier handling as well as potential wide-range distribution due to large scale cyclotron based production of ^{18}F. Furthermore, spatial resolution might be improved by a lower positron range (38). However, compared to literature using ^{68}Ga-PSMA-11, our results do not reveal significant diagnostic improvements. Moreover, compared with ^{18}F-PSMA-1007 and ^{18}F-DCFPyl, potential benefits may arise from the radiohybrid concept facilitating the use of ^{68}Ga and therapeutic nuclides

offering both ^{68}Ga-based imaging for remote location using a generator as well as exploiting the applications for theranostics (e.g. exact pre-therapy PET-dosimetry for treatment planning).

Our analysis has limitations. First, it was conducted in a retrospective manner in a limited number of patients. Second, we had to restrict the analyses to a template-based approach as single lymph node correlations between imaging and surgery are not feasible. However, this was performed in a rigorous fashion and provides substantial evidence for future prospective trials. Third, PSMA immunohistochemistry was not performed for lymph node metastases. However, for N-staging, routine H&E staining is usually sufficient. Only in cases of a second primary tumor would PSMA-immunohistochemistry be helpful to investigate its etiology. Fourth, as this analysis was primarily intended to investigate the potential of ^{18}F-rhPSMA-7 for N-staging, no detailed analysis of its potential for describing the intraprostatic tumor extent or distant disease has been performed. Fifth, given the approach that only patients who subsequently underwent surgery were included in the study, the potential of ^{18}F-rhPSMA-7 to detect organ (e.g. bone) metastases could not be investigated in this analysis.

CONCLUSIONS

^{18}F-rhPSMA-7 PET provides superior N-staging of high-risk primary PC compared with morphological imaging. The efficacy of ^{18}F-rhPSMA-7 is similar to that of published data for ^{68}Ga-PSMA-11 and offers the additional logistical and economic advantages of radio-fluorination.

KEY POINTS:

Question: What is the diagnostic efficacy of ^{18}F-rhPSMA-7 in N-staging of high-risk prostate cancer in the primary setting?

Pertinent Findings: This retrospective study showed that ^{18}F-rhPSMA-7 PET provides superior N-staging of high-risk primary prostate cancer compared with morphological imaging. The efficacy of ^{18}F-rhPSMA-7 is similar to that of published data for ^{68}Ga-PSMA-11 and offers the additional logistical and economic advantages of radio-fluorination.

Implications for Patient Care: ^{18}F-rhPSMA-7 PET can significantly improve primary N-staging.

REFERENCES

1. Torre LA, Bray F, Siegel RL, Ferlay J, Lortet-Tieulent J, Jemal A. Global cancer statistics, 2012. CA Cancer J Clin. 2015;65:87-108.

2. Cheng L, Zincke H, Blute ML, Bergstralh EJ, Scherer B, Bostwick DG. Risk of prostate carcinoma death in patients with lymph node metastasis. Cancer. 2001;91:66-73.

3. Mottet N, Bellmunt J, Briers E, et al. EAU - ESTRO - ESUR - SIOG Guidelines on prostate cancer. 2017 update. EAU Guidelines Edn presented at the EAU Annual Congress Copenhagen 2018 ISBN 978-94-92671-01-1. 2018.

4. Kothari PS, Scardino PT, Ohori M, Kattan MW, Wheeler TM. Incidence, location, and significance of periprostatic and periseminal vesicle lymph nodes in prostate cancer. Am J Surg Pathol. 2001;25:1429-1432.

5. Danella JF, deKernion JB, Smith RB, Steckel J. The contemporary incidence of lymph node metastases in prostate cancer: implications for laparoscopic lymph node dissection. J Urol. 1993;149:1488-1491.

6. Partin AW, Mangold LA, Lamm DM, Walsh PC, Epstein JI, Pearson JD. Contemporary update of prostate cancer staging nomograms (Partin Tables) for the new millennium. Urology. 2001;58:843-848.

7. Gervasi LA, Mata J, Easley JD, et al. Prognostic significance of lymph nodal metastases in prostate cancer. J Urol. 1989;142:332-336.

8. Campbell SC, Klein EA, Levin HS, Piedmonte MR. Open pelvic lymph node dissection for prostate cancer: a reassessment. Urology. 1995;46:352-355.

9. Briganti A, Blute ML, Eastham JH, et al. Pelvic lymph node dissection in prostate cancer. Eur Urol. 2009;55:1251-1265.

10. Briganti A, Abdollah F, Nini A, et al. Performance characteristics of computed tomography in detecting lymph node metastases in contemporary patients with prostate cancer treated with extended pelvic lymph node dissection. Eur Urol. 2012;61:1132-1138.

11. Evangelista L, Guttilla A, Zattoni F, Muzzio PC, Zattoni F. Utility of choline positron emission tomography/computed tomography for lymph node involvement identification in intermediate- to high-risk prostate cancer: a systematic literature review and meta-analysis. Eur Urol. 2013;63:1040-1048.

12. Corfield J, Perera M, Bolton D, Lawrentschuk N. (68)Ga-prostate specific membrane antigen (PSMA) positron emission tomography (PET) for primary staging of high-risk prostate cancer: a systematic review. World J Urol. 2018;36:519-527.

13. Perera M, Papa N, Christidis D, et al. Sensitivity, specificity, and predictors of positive (68)Ga-prostate-specific membrane antigen eositron Emission tomography in advanced prostate cancer: A systematic review and meta-analysis. Eur Urol. 2016;70:926-937.

14. Giesel FL, Hadaschik B, Cardinale J, et al. F-18 labelled PSMA-1007: biodistribution, radiation dosimetry and histopathological validation of tumor lesions in prostate cancer patients. Eur J Nucl Med Mol Imaging. 2017;44:678-688.

15. D'Amico AV, Whittington R, Malkowicz SB, et al. Biochemical outcome after radical prostatectomy, external beam radiation therapy, or interstitial radiation therapy for clinically localized prostate cancer. JAMA. 1998;280:969-974.

16. Souvatzoglou M, Eiber M, Martinez-Moeller A, et al. PET/MR in prostate cancer: technical aspects and potential diagnostic value. Eur J Nucl Med Mol Imaging. 2013;40 Suppl 1:S79-88.

17. Eiber M, Maurer T, Souvatzoglou M, et al. Evaluation of hybrid ^{68}Ga-PSMA ligand PET/CT in 248 patients with biochemical recurrence after radical prostatectomy. J Nuc Med. 2015;56:668-674.

18. Heck MM, Retz M, Bandur M, et al. Topography of lymph node metastases in prostate cancer patients undergoing radical prostatectomy and extended lymphadenectomy: results of a combined molecular and histopathologic mapping study. Eur Urol. 2014;66:222-229.

19. Maurer T, Souvatzoglou M, Kubler H, et al. Diagnostic efficacy of [11C]choline positron emission tomography/computed tomography compared with conventional computed tomography in lymph node staging of patients with bladder cancer prior to radical cystectomy. Eur Urol. 2012;61:1031-1038.

20. DeLong ER, DeLong DM, Clarke-Pearson DL. Comparing the areas under two or more correlated receiver operating characteristic curves: a nonparametric approach. Biometrics. 1988;44:837-845.

21. Obuchowski NA. Nonparametric analysis of clustered ROC curve data. Biometrics. 1997;53:567-578.

22. Smith PJ, Hadgu A. Sensitivity and specificity for correlated observations. Stat Med. 1992;11:1503-1509.

23. Zeger SL, Liang KY. Longitudinal data analysis for discrete and continuous outcomes. Biometrics. 1986;42:121-130.

24. Team RC. A language and environment for statistical computing. R Foundation for Statistical Computing. https://www.R-project.org/, accessed 30 October 2019.

25. Robin X, Turck N, Hainard A, et al. pROC: an open-source package for R and S+ to analyze and compare ROC curves. BMC Bioinformatics. 2011;12:77.

26. Halekoh U, Hojsgaard S, Yan J. The R package geepack for generalized estimating equations. J Stat Softw. 2006;15:1-11.

27. Hovels AM, Heesakkers RA, Adang EM, et al. The diagnostic accuracy of CT and MRI in the staging of pelvic lymph nodes in patients with prostate cancer: a meta-analysis. Clin Radiol. 2008;63:387-395.

28. Tiguert R, Gheiler EL, Tefilli MV, et al. Lymph node size does not correlate with the presence of prostate cancer metastasis. Urology. 1999;53:367-371.

29. Heesakkers RA, Hovels AM, Jager GJ, et al. MRI with a lymph-node-specific contrast agent as an alternative to CT scan and lymph-node dissection in patients with prostate cancer: a prospective multicohort study. Lancet Oncol. 2008;9:850-856.

30. Afshar-Oromieh A, Haberkorn U, Eder M, Eisenhut M, Zechmann CM. [68Ga]Gallium-labelled PSMA ligand as superior PET tracer for the diagnosis of prostate cancer: comparison with 18F-FECH. Eur J Nucl Med Mol Imaging. 2012;39:1085-1086.

31. Maurer T, Gschwend JE, Rauscher I, et al. Diagnostic efficacy of (68)Gallium-PSMA positron emission tomography compared to conventional imaging for lymph node staging of 130 consecutive patients with intermediate to high risk prostate cancer. J Urol. 2016;195:1436-1443.

32. Hope TA, Goodman JZ, Allen IE, Calais J, Fendler WP, Carroll PR. Meta-analysis of (68)Ga-PSMA-11 PET accuracy for the detection of prostate cancer validated by histopathology. J Nucl Med. 2019;60:786-793.

33. von Eyben FE, Picchio M, von Eyben R, Rhee H, Bauman G. (68)Ga-Labeled prostate-specific membrane antigen ligand positron emission tomography/computed tomography for prostate cancer: A systematic review and meta-analysis. Eur Urol Focus. 2018;4:686-693.

34. Gorin MA, Rowe SP, Patel HD, et al. Prostate specific membrane antigen targeted (18)F-DCFPyL positron emission tomography/computerized tomography for the preoperative staging of high risk prostate cancer: Results of a prospective, phase II, single center study. J Urol. 2018;199:126-132.

35. Farolfi A, Gafita A, Calais J, et al. (68)Ga-PSMA-11 positron emission tomography detects residual prostate cancer after prostatectomy in a multicenter retrospective study. J Urol. 2019:In press.

36. Maurer T, Robu S, Schottelius M, et al. (99m)Technetium-based prostate-specific membrane antigen-radioguided surgery in recurrent prostate cancer. Eur Urol. 2019;75:659-666.

37. Jilg CA, Drendel V, Rischke HC, et al. Diagnostic accuracy of Ga-68-HBED-CC-PSMA-ligand-PET/CT before salvage lymph node dissection for recurrent prostate cancer. Theranostics. 2017;7:1770-1780.

38. Cho ZH, Chan JK, Ericksson L, et al. Positron ranges obtained from biomedically important positron-emitting radionuclides. J Nucl Med. 1975;16:1174-1176.

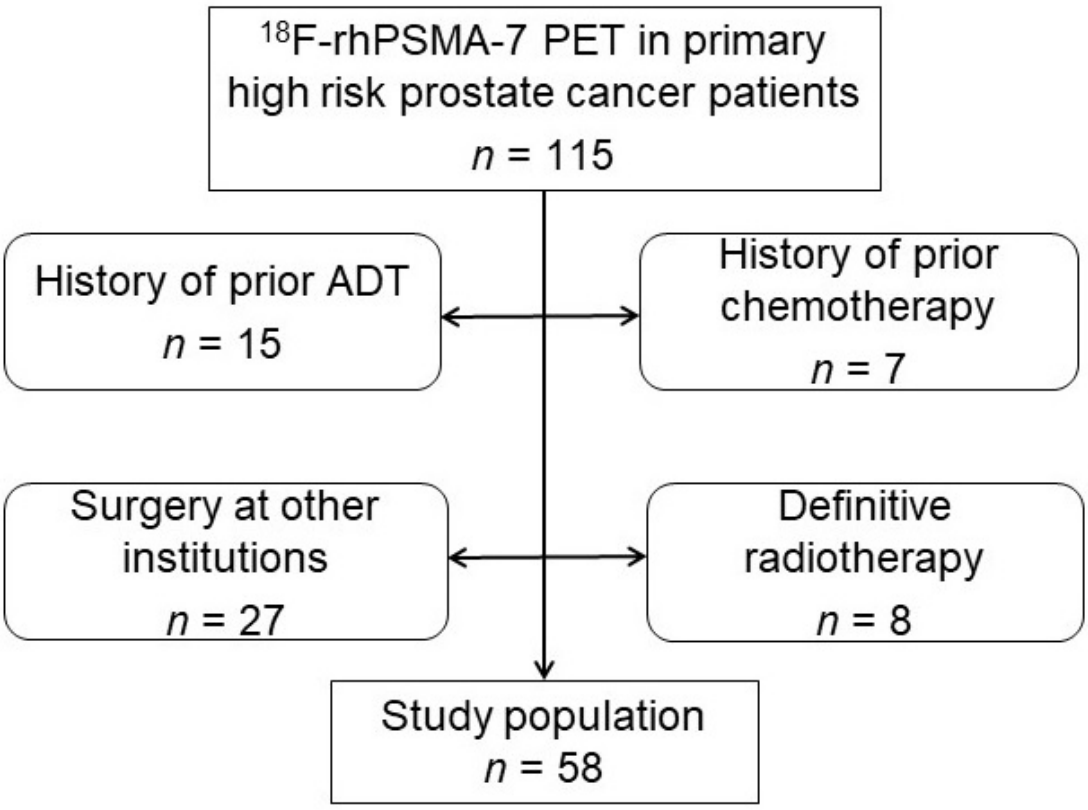

Fig. 1 Flow chart of patient selection.

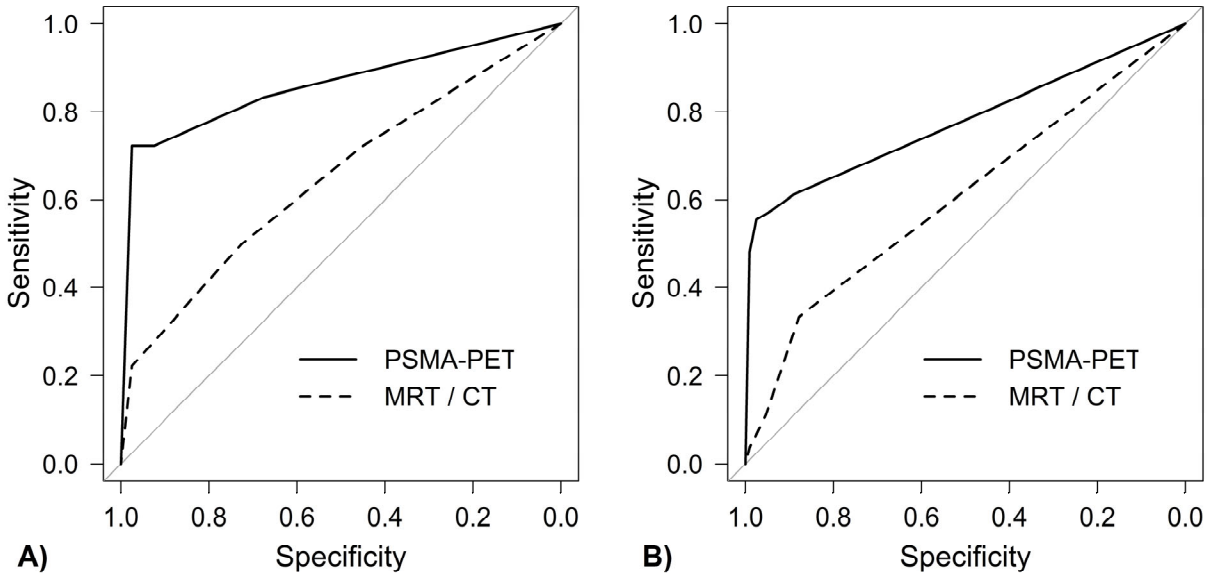

Fig. 2 ROC curves for ^{18}F-rhPSMA-7 PET (solid line) and morphological imaging (CT / MRI) (dashed line) for primary lymph node staging prostate cancer in a patient- (A) and template-based analysis (B); comparison to AUC=0.5 (grey line)).

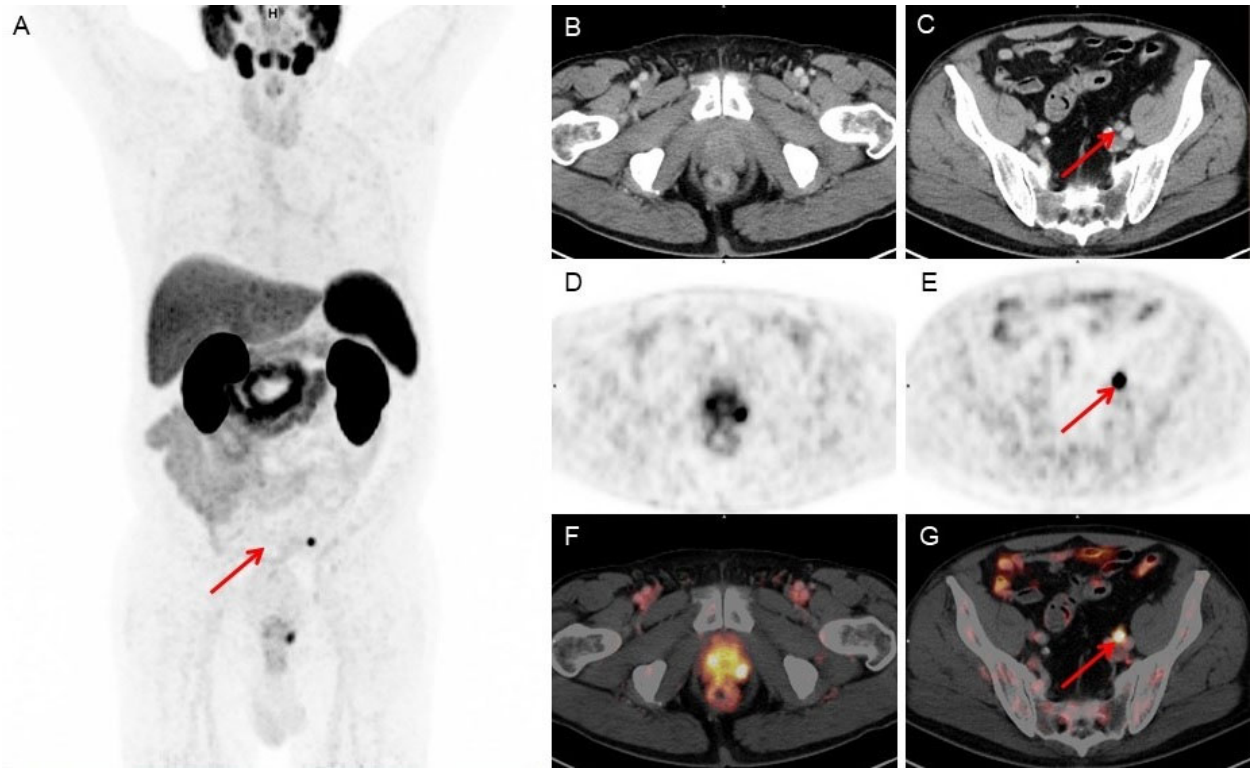

Fig. 3 Set of images from a 71-year-old patient (Gleason Score 10, iPSA 1.15 ng/mL). The whole body MIP (maximum-intensity-projection, A) displays the local tumour and one suspicious lesion (red arrow). The local tumour is not detectable in the CT images (B), but shows increased tracer uptake in the ^{18}F-rhPSMA-7 PET and fused PET/CT images (C, D). CT images (E) reveal a suspicious finding with an 8 mm lymph node ventral of the left external iliac vein. Corresponding ^{18}F-rhPSMA-7 PET (F) and fused PET/CT images (G) show an intense uptake with a high lesion-to-background ratio in this small lymph node indicating a lymph node metastasis. Radical prostatectomy with extended pelvic lymph node dissection confirmed a single lymph node metastasis.

Table 1. Patient characteristics.

Characteristic	
Total	
N (%)	58 (100)
Age, y[1]	
Mean	67.7
Median	68
IQR	65–73
Range	48–80
PSA, ng/mL[1]	
Mean	18.1
Median	12.2
IQR	7.3–22.4
Range	1.2–81.6
Gleason Score, n (%)	
7a	11 (19.0)
7b	25 (43.1)
8	4 (6.9)
9	18 (31.0)
10	0
Pathological T-stage, n (%)	
≤ pT2c	26 (44.8)
pT3a	12 (20.7)
≥ pT3b	20 (34.5)
Pathological N-stage	
pN0	40 (69)
pN1	18 (31)
Lymph nodes removed	
N	1137
Median	18
IQR	8
Range	8-53
Lymph nodes with metastasis	
N	71
Median	0
IQR	1
Range	0-15
Injected activity, MBq	
N	327.7
Median	327
IQR	306.5–363
Range	132–410
Uptake time, min	
N	82
Median	79.5
IQR	70-87.25
Range	60-153

IQR, interquartile range; RPX: radical prostatectomy.

[1]At time of imaging.

Table 2. Diagnostic accuracy of ^{18}F-rhPSMA-7 PET and cross-sectional imaging compared with histology (patient-based analysis).

Morphological Grading	Histology: LN metastasis		
	pos.	neg.	
1†	4	1	PPV: 72.5%
2†	0	0	
3†	5	10	
4	4	11	NPV: 76.3%
5	5	18	
Total	18	40	58
	Sens.: 50.0%	Spec.: 72.5%	Acc.: 65.5%

^{18}F-rhPSMA7-PET Grading	Histology: LN metastasis		
	pos.	neg.	
1*	13	1	PPV: 81.3%
2*	0	2	
3	1	5	NPV: 88.1%
4	1	5	
5	3	27	
Total	18	40	58
	Sens.: 72.2%	Spec.: 92.5%	Acc.: 86.2%

(pos.: positive; neg.: negative; Sens.: sensitivity; Spec.: specificity; PPV: positive predictive value; NPV: negative predictive value; Acc.: accuracy; LN: lymph nodes; †: values for Morphological grading: 1–3 positive (4–5 negative) **, *: values for ^{18}F-rhPSMA-7 PET Grading: 1+2 positive (3–5: negative) for LN metastasis**)

** based on highest Youden index

Table 3. Diagnostic accuracy of ^{18}F-rhPSMA-7 PET and cross-sectional imaging compared with histology (template-based analysis).

Morphological Grading	Histology: LN metastasis		
	pos.	neg.	
1†	1	4	PPV: 28.8%
2†	0	0	
3†	4	12	
4	11	25	NPV: 86.7%
5	36	282	
Total	52	323	375
	Sens.: 9.6%	Spec.: 95.0%	Acc.: 83.2%

^{18}F-rhPSMA7-PET Grading	Histology: LN metastasis		
	pos.	neg.	
1*	24	5	PPV: 73.7%
2*	4	5	
3	1	10	NPV: 92.9%
4	2	17	
5	21	286	
Total	52	323	375
	Sens.: 53.8%	Spec.: 96.9%	Acc.: 90.9%

(pos.: positive; neg.: negative; Sens.: sensitivity; Spec.: specificity; PPV: positive predictive value; NPV: negative predictive value; Acc.: accuracy; LN: lymph nodes; †: values for Morphological grading: 1–3 positive (4–5 negative**), *: values for ^{18}F-rhPSMA-7 PET Grading: 1+2 positive (3–5: negative) for LN metastasis**)

** based on highest Youden index

Supplemental information

The following definitions were used for the image reading:

In PET the following criteria were used: 1: tumor manifestation (intense, focal ^{18}F-rhPSMA-7 uptake higher than liver), 2: probably tumor manifestation (^{18}F-rhPSMA-7 uptake clearly higher than background in vessels, but not higher than liver), 3: equivocal (^{18}F-rhPSMA-7 faint uptake between background in muscle and vessels), 4: probably benign (^{18}F-rhPSMA-7 uptake as faint as background, e.g. equally to adjacent muscle), 5: benign (no ^{18}F-rhPSMA-7 uptake). Hereby, anatomical images were only used for anatomical allocation of a suspicious focal increased uptake to the corresponding LN field.

In morphological imaging the following criteria were used: 1: tumor manifestation (short axis diameter > 10mm), 2: probably tumor manifestation (short axis diameter 8-10 mm, round configuration and/or regional grouping), 3: equivocal (short axis diameter 8-10 mm, oval configuration and no regional grouping), 4: probably benign (short axis diameter < 8mm), 5: benign (short axis diameter < 5mm).

Supplemental table 1. Performance of ^{68}Ga-PSMA-11 PET according to literature

Literature	**Sensitivity**	**Specificity**	**PPV**	**NPV**	**ACC**	**N=**
Hope et al 2018	74	96	93	85	86	266
v. Eyben et al 2016	61	97				273
Corfield et al 2018	33–92	64–91	83–96	80–96		216
Perera et al 2016	86	86				239
Our Results	72	93	74	93	93	58

Supplemental table 2

Diagnostic accuracy of ^{18}F-rhPSMA-7 PET and cross-sectional imaging compared with histology (template-based analysis) modified by data retrieved from follow up.

Morphological Grading	Histology: LN metastasis		
	pos.	neg.	
1†	2	3	PPV: 28.6%
2†	0	0	
3†	4	12	
4	12	24	NPV: 86.4%
5	36	282	
Total	54	321	375
	Sens.: 11.1%	Spec.: 95.3%	Acc.: 83.2%

^{18}F-rhPSMA7-PET Grading	Histology: LN metastasis		
	pos.	neg.	
1*	26	3	PPV: 78.9%
2*	4	5	
3	1	10	NPV: 92.9%
4	2	17	
5	21	286	
Total	54	321	375
	Sens.: 55.6%	Spec.: 97.5%	Acc.: 91.4%

(pos.: positive; neg.: negative; Sens.: sensitivity; Spec.: specificity; PPV: positive predictive value; NPV: negative predictive value; Acc.: accuracy; LN: lymph nodes; †: values for Morphological grading: 1–3 positive (4–5 negative**), *: values for 18F-rhPSMA-7 PET Grading: 1+2 positive (3–5: negative) for LN metastasis**)

** based on highest Youden index

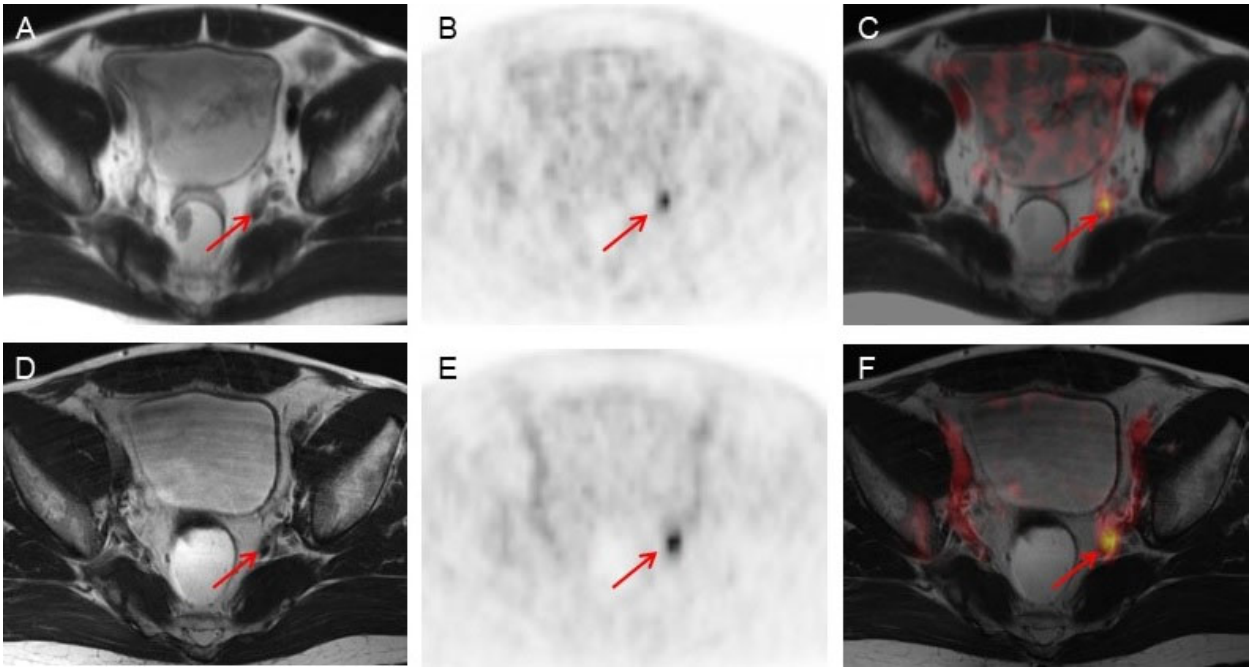

Supplemental Fig. 1: Pre- (lower row) and 7 months postoperative (upper row) ^{18}F-rhPSMA-7 PET/MR datasets from a 61-year-old patient (Gleason Score 9, iPSA 25.98 ng/mL). Preoperative staging shows an ^{18}F-rhPSMA-7-positive lymph node in the left pelvic. After surgery PSA persistence at a PSA value of 0.21 ng/ml was noted. ^{18}F-rhPSMA-7 PET/MR imaging revealed the lymph node metastasis still in place which was subsequently successfully removed using PSMA-targeted radio-guided surgery.